

# Dynamics of Elastic Boundaries

Sharad Ramanathan and Alexander E. Lobkovsky

*Institute for Theoretical Physics, University of California, Santa Barbara, CA 93106*

(July 19, 2017)

We study, both analytically and numerically, the dynamics of elastic boundaries such as crack fronts in fracture and surfaces of contact in solid on solid friction. The elastic waves in the solid give rise to kinks that move with a characteristic velocity along the boundary. As stopping kinks pass through they cause moving parts of the boundary to stop. Starting kinks cause stationary parts of the boundary to move. We study the interaction of these kinks with disorder that arises from the spatial variations of the friction constant or fracture energy. In the absence of elastic waves, elastic boundaries with disorder operate at a critical point leading to a power-law distribution of slip events and self-affine boundaries. Elastic waves result in relevant perturbations at this fixed point. Slip events beyond a critical size run away and the velocity of the boundary jumps to a nonzero value when the external load is increased above a threshold. We analyze in detail a class of simple models that capture the essential features of bulk vectorial elasticity and discuss the implications of our results for friction and fracture dynamics.

Moving elastic boundaries occur in a wide range of problems. Examples are the interface of contact in solid on solid friction, the crack front in fracture, or the line of contact in the case of peeling of an elastic film off a substrate. There remain several unsolved puzzles. For instance, why the frequency of the earthquakes averaged over all faults is proportional to a power of the seismic moment [1], while some faults show an excess of large events. Power law statistics of slip events may imply that the boundary is rough on all length scales just before it begins to move. Experiments on cracks restricted to move in a plane between two pressure welded Plexiglas sheets find that the crack front is self affine near onset of fracture [2]. The dynamics of an earthquake fault during a single slip event has received much attention since the inversion of seismic data by Heaton [3] discovered slip bands of finite spatial extent. Nielsen *et al* [4] found corroborating numerical evidence in simulations of faults with rate and state dependent friction. Both studies use acoustic models, neglecting the vectorial elastodynamics of the bulk. Details of how these slip bands arise and how earthquakes start and stop are yet poorly understood.

Analytic progress in problems with moving elastic boundaries is difficult and numerical simulations are intensive. Fisher and collaborators [5] considered a class of models to study rupture along heterogeneous earthquake faults. These were found to naturally operate at a critical point leading to power-law scaling of earthquake statistics. They also considered dynamical effects arising due to friction laws and elastic waves in an acoustic model. A variety of other simplified models to study the dynamics of boundaries omit some important features such as long range elasticity [6], bulk elastic waves [7] and the vectorial nature of the problem [5,8]. To reproduce the complexity in the dynamics of friction for instance, the transition between stick slip and steady sliding, Carlson and Batista introduced complicated friction laws [9].

In this letter, we show that vectorial elastodynamics of the bulk results in complex friction dynamics even when the boundary obeys Coulomb friction. We find kink solutions that move along the boundary with a specific velocity and identify generic features of the equations of motion for elastic boundaries that would support such solutions. To understand the interactions of kinks with heterogeneities, we study a class of models, in the spirit of Re f. [5], which capture the effects of elastodynamics. In our models, these kinks qualitatively alter the dynamics of the boundary near the onset of motion.

To motivate our study, let us consider the problem of an elastic solid sliding on and always in contact with a flat infinitely rigid substrate. Let  $\hat{y}$  be normal to the substrate and  $\hat{z}$  be the direction of sliding. We study a two dimensional problem by requiring translational invariance along the  $\hat{x}$  direction. Let  $f(z, t)$  be the displacement in the  $z$  direction of the solid's boundary relative to the substrate. An external shear stress  $\sigma_{yz}^\infty = T$  and a normal load  $\sigma_{yy}^\infty = P$  are applied far away. We obtain an effective equation of motion for  $f(z, t)$  by requiring that on the boundary,

$$\begin{cases} \sigma_{yz} = \mu \sigma_{yy}, & \text{when the solid is sliding, } \dot{f} > 0, \\ \sigma_{yz} < \mu \sigma_{yy}, & \text{when it is stuck, } \dot{f} = 0. \end{cases} \quad (1)$$

(Note that the solid can slide only in the positive  $z$  direction, hence  $\dot{f} \geq 0$ ). We assume that the friction coefficient  $\mu$  is independent of slip or sliding velocity [10]. Given  $f(z, t)$  and that elastic waves that radiate into the bulk are not reflected back, one can solve the equations of elastodynamics to obtain the resulting stresses at the boundary. Then, Eq. (1) becomes

$$\frac{1}{2} \frac{\partial f(z, t)}{\partial t} = \Sigma(z, t) \Theta(\Sigma(z, t)), \quad (2a)$$

where,

$$\Sigma(z, t) = \int_{z', t' < t} dz' dt' J(z - z', t - t') \frac{\partial f(z', t')}{\partial t'} + T - \gamma, \quad (2b)$$

with  $\gamma = \mu P$ , and  $J = J_{\text{friction}} = J_{yz} - \mu J_{yy}$ , where

$$J_{yz} = \delta'(z) + \frac{1}{2\pi} \frac{\partial}{\partial t} \begin{cases} \frac{1}{t} \frac{\sqrt{1 - z^2/\kappa t^2}}{1 - \sqrt{1 - z^2/t^2} \sqrt{1 - z^2/\kappa t^2}}, & \text{for } 0 \leq |z|/t < 1 \\ \frac{\sqrt{1 - z^2/\kappa t^2}}{t[1 + (z^2/t^2 - 1)(1 - z^2/\kappa t^2)]}, & \text{for } 1 < |z|/t < \sqrt{\kappa}, \end{cases} \quad (3)$$

and

$$J_{yy} = \frac{1}{2\pi t} \frac{\partial}{\partial z} \left[ \frac{z/t \sqrt{z^2/t^2 - 1} \sqrt{1 - z^2/\kappa t^2}}{1 + (z^2/t^2 - 1)(1 - z^2/\kappa t^2)} \right], \quad \text{for } 1 < |z|/t < \sqrt{\kappa}. \quad (4)$$

Here  $\kappa$  is the square of the ratio of the longitudinal to the transverse bulk wave speeds. A plot of the friction kernel  $J_{\text{friction}}$  as a function of time  $t$  at a fixed  $z$  is shown in Figs. 1 (c) and (d).

When  $T > \gamma$ , there exists a unique steady [11] state with the whole boundary moving at a constant velocity. We now seek, for  $T < \gamma$ , steady state solutions of Eq. (2),  $f(z, t) = F(z - st) = F(\xi)$ . Substitution into Eq. (2) with  $J = J_{\text{friction}}$  yields

$$\left\{ A(s)F'(\xi) + B(s) \mathcal{P} \int \frac{F(\xi')}{(\xi - \xi')^2} d\xi' + T - \gamma \right\} \Theta[-sF'(\xi)] = 0, \quad (5)$$

where  $\mathcal{P}$  denotes the Cauchy principal value and prime denotes derivative with respect to  $\xi$ . The coefficients in Eq. (5) are given by

$$A(s) = \mu - \frac{s^2 \text{sign}(s)(1 - s^2/\kappa)\sqrt{s^2 - 1} - \mu s^2}{2[1 + (s^2 - 1)(1 - s^2/\kappa)]} \quad (6)$$

$$B(s) = -\frac{s^2 \sqrt{1 - s^2/\kappa} [\mu \text{sign}(s)\sqrt{s^2 - 1} + 1]}{2\pi[1 + (s^2 - 1)(1 - s^2/\kappa)]}. \quad (7)$$

We have shown [12] that a solution to Eq. (5) exists if and only if there exists  $s_0$  such that  $B(s_0) = 0$ . Steady state solutions can therefore propagate only when  $\mu > \mu_c = 1/\sqrt{\kappa - 1}$  and at a velocity  $s_0 = -\sqrt{1 + 1/\mu^2}$ . Furthermore, since  $s_0$  is negative, the expression in the curly brackets in Eq. (5) must vanish when  $F' > 0$ . For loads below threshold, i.e.,  $T < \gamma$ , we find a steady state solution of the form

$$F'(\xi) = \frac{\gamma - T}{A(s_0)} \Theta(\xi). \quad (8)$$

This is a starting kink moving in the negative  $z$  direction. A stopping kink  $F'(\xi) = \frac{\gamma - T}{A(s_0)} [1 - \Theta(\xi)]$ , and pulses,  $F'(\xi) = \frac{\gamma - T}{A(s_0)} [\Theta(\xi) - \Theta(\xi - a)]$ , of any width  $a$  are also solutions. These predictions are confirmed by our numerics.

These kink solutions are stable. When the speed of the backward moving kink  $|s| > |s_0|$ ,  $B > 0$  and the integral term in Eq. (5) diverges logarithmically at the kink tip,  $\xi = 0$ , so as to slow it down. If, on the other hand,  $|s| < |s_0|$  the same term diverges with the opposite sign speeding up the kink.

The motion of a planar crack through a three dimensional elastic solid is also described by Eq. (2) with  $J = J_{\text{fracture}}(z, t)$  sketched in Fig. 1 (d). Here,  $f(z, t)$  is the shape of the crack front. The equation of motion is the statement that the local elastic energy flux to the crack tip is spent to create new surfaces there. The driving force  $T$  is related to the external loads and  $\gamma$  is the surface energy [13]. Here again we find starting and stopping kinks that move with a characteristic velocity. Unlike in the case of friction, these kinks move in either direction along the crack front.

Further progress can be made by realizing that the motion of elastic boundaries is generically described by Eq. (2). It possesses several remarkable features that arise due to the elastodynamics of the bulk and lead to the existence of steady state kinks. First, the equation for the motion of the boundary is first order in time. Second, the kernels  $J(z, t)$  have the following properties: (i)  $J(z, t < |z|/c) = 0$ , where  $c$  is the longitudinal wave velocity, (ii) the kernel

is homogeneous degree  $-2$ , so that  $J(z, t) = \frac{j(z/t)}{z^2}$  with  $j(0) = 1$ , and (iii)  $J$  is non-monotonic as a function of  $t$  at all  $z$ . In particular, at a fixed  $z$ ,  $J$  is negative for some period after the arrival of the longitudinal sound wave and then changes sign [14]. This change of sign implies there exists a speed  $s_0 < c$  such that for all  $z$

$$\int_{|z|/c}^{|z|/s_0} J(z, t') dt' = 0 \quad (9)$$

when  $J(z, t) = J(-z, t)$ . The equation (9) is a sufficient condition for steady kink solutions that move with speed  $s_0$  in either direction to exist.<sup>1</sup> To see that, we first note that condition (ii) implies that the steady state equation (5) is generally valid. Furthermore, we can rigorously show that condition (9) implies that  $B(s_0) = 0$ . Thus steady state kink solutions exist for all such kernels.

The detailed form of kernels that arise in problems of moving elastic boundaries depend on various parameters such as the microscopic time and length scales, and also on reflection of waves from free surfaces, etc. We would like to consider a simple model that captures effects of vectorial elastodynamics to understand the interaction of the kinks with disorder near the onset of motion. We therefore study a model kernel, shown in Fig. 1 (a),

$$J_{\text{model}} = \frac{1}{z^2} [-\Theta(t - |z|) + (2 + \alpha)\Theta(c_1 t - |z|) - \alpha\Theta(c_2 t - |z|)], \quad (10)$$

with  $1 > c_1 > c_2$ . At a fixed position  $z$  this model kernel is zero until time  $t = |z|$ . In the time interval  $t \in (|z|, |z|/c_1)$  it is equal to  $-1/z^2$ . It then jumps to  $(\alpha + 1)/z^2$  until time  $t = |z|/c_2$  at which it settles down to its static value of  $1/z^2$ .

For  $T < \gamma$ , the equation of motion (2), with the model kernel, admits starting and stopping kinks that move in both directions. Their velocity can be calculated using equation (9). It is

$$s_0 = \begin{cases} \frac{c_1(\alpha + 1)}{\alpha + 2 - c_1^2}, & \text{for } (\alpha + 1)(c_1 - c_2) > c_2(1 - c_1) \\ \frac{1}{2 + \alpha - c_1 - \alpha c_1/c_2}, & \text{otherwise.} \end{cases} \quad (11)$$

This is indeed confirmed by our numerics.

Let us now turn to the effects of disorder which arises due to spatially varying material properties, such as the coefficient of friction or the surface energy. We introduce disorder by making  $\gamma$  in Eq. (2) position dependent. It is important to note that in general, the function  $\gamma$  depends both on the coordinate  $z$  along the boundary as well as the position of the boundary  $f(z, t)$ . In our simulations, the variable  $\gamma(z, f)$  is uniformly distributed in  $[0, \Gamma]$ . All lengths are measured in units of the correlation length of  $\gamma$ .

We study Eq. (2) numerically by a finite difference method. Let us first consider the case the model kernel with  $\alpha = 0$ . We increase the external driving force in small increments from zero. These increments are chosen in such a way as to dislodge the most weakly pinned point of the boundary. Avalanches begin with two starting kinks that nucleate there and move outward until they encounter a tough patch. Stopping kinks are then nucleated and move inward until the boundary is arrested stopping the avalanche. The dynamic exponent  $z$  is defined by the duration  $\tau \sim \ell^z$  of an avalanche of size  $\ell$ . The avalanches show a power law distribution up to a characteristic length  $\xi_-$  with longer avalanches being much rarer. Below the length scale  $\xi_-$  the boundary is self affine with  $\langle |f(z, t) - f(z', t)|^2 \rangle \sim |z - z'|^{2\zeta}$ , which defines the roughness exponent,  $\zeta$ . As the load approaches the critical load,  $T_t^{\text{qs}}$ ,  $\xi_-$  diverges as  $(T_t^{\text{qs}} - T)^{-\nu}$ , defining the correlation exponent,  $\nu$ . Above this load, the boundary as a whole begins to move with an average velocity,  $v \sim (T - T_t^{\text{qs}})^\beta$ ,  $\beta$  being the velocity exponent.

The Eq. (2) has been studied extensively for a quasistatic model where sound waves in the bulk are neglected, so that  $J = J_{\text{qs}}(z, t) = 1/z^2$  [15]. Note that  $J_{\text{model}}(\alpha = 0) \leq J_{\text{qs}}$  for all  $z$  and  $t$ , and for  $t > 1/c_2$ , the two are equal. The no-passing rule [16] implies that the static exponents  $\zeta$  and  $\nu$  are the same in both cases. For the quasistatic model, the physics is determined by a critical fixed point and a  $2 - \varepsilon$  renormalization group calculation yields, with  $\varepsilon = 1$ ,  $\zeta = 1/3$ ,  $\nu = 3/2$ . The dynamic exponents for our model are different from the quasistatic model and a renormalization group calculation yields the dynamic exponent,  $z = 1$  and  $\beta = 1$ . These results agree with our numerics, and the results are shown in Figs. 2 and 3.

We find that for  $\alpha > 0$  the structure of avalanches is the same as before for small enough loads. The typical avalanche size increases with the load. When it reaches a critical value  $\ell_c$  determined by the parameters  $\alpha$ ,  $c_1$  and  $c_2$ ,

---

<sup>1</sup>When the kernel is asymmetric, kinks may only move in one direction, as in the case of friction.

the starting kinks zip through the whole system causing it to move. We make this inference from the fact that the threshold load  $T_t(\alpha, c_1, c_2)$ , is lower than that for the quasistatic kernel  $T_t^{qs}$  and that

$$T_t^{qs} - T_t(\alpha, c_1, c_2) \sim \alpha^{3/2}(c_1 - c_2)g(c_1), \quad (12)$$

as shown in Fig. (4). This scaling form of the suppression of the threshold load is in agreement with our analytical results [12]. Thus, as in the acoustic models in Refs. [5,17], we expect a power law distribution of small events with the same power law as the quasistatic model combined with characteristic system size events. Also the velocity jumps to a finite value at  $T = T_t(\alpha, c_1, c_2)$  as shown in Fig. 3. From our study we expect qualitatively similar behavior near threshold in the case of friction and fracture.

In conclusion, we have demonstrated that vectorial elasticity of the bulk must be taken into account in order to properly describe dynamics of elastic boundaries. Specifically, steadily propagating kinks arise naturally in elastodynamic models. Pulse solutions propagating with a specific velocity, where parts of the boundary are moving can be constructed from starting and stopping kinks. Spatial width of the pulse solutions is arbitrary and must be set by some nonlinearity in the system or the reflection of waves from free boundaries. These pulse solutions should be observable in experiments on fracture similar to those of Schmittbuhl [2]. These kinks can presumably be triggered at an edge of the sample. Simulations of solid on solid friction including the bulk elastodynamics [18] suggest that the key features of the kernels obtained from a continuum treatment persist and hence kinks solutions must still exist though the velocity of motion of these kinks will be determined by the detailed shape of the kernel. Preliminary results indicate that the effects of sound damping in the bulk is to set a spatial extent for the pulses, but the details remain to be explored. More complicated friction laws, such as different static and dynamic friction coefficients, lead to complex behavior left for future studies. However, we expect kink solutions and the qualitative threshold behavior to persist.

In systems with disorder, the dynamics near the onset of motion is controlled by nucleation of starting kinks by weak patches and of stopping kinks by tougher regions. Once an avalanche reaches a critical size which is set by the details of the kernel, it runs away spanning the entire system. Therefore, there should be an excess of system size avalanches beyond the crossover scale. Even when one includes the finite response time of a point on the boundary to changes in the stress, the same physics persists. Since avalanches beyond a critical size run away, rare weak patches should play an important role that has yet to be explored.

In this letter we restricted our attention to one dimensional boundaries. When the spatial dimensionality of the boundary is two, "kink-on-kink" solutions arise. Thus, a possible mechanism for stopping a spreading circular earthquake, is a stopping kink-on-kink that propagates around the earthquake front. Questions about the dynamics of these kinks as well as their interaction with disorder remain open. However, models in which kinks are featured as the fundamental excitations offer significant advantages over full scale three dimensional numerical simulations and should be studied.

We would like to thank Daniel S. Fisher, Jim Rice, Jean Carlson and Jim Langer for extensive discussions. This work was supported by National Science Foundation via PHY94-07194 and DMR-9510394. AL wishes to acknowledge support of the Department of Energy via grant No. DE-FG03-84ER45108.

- 
- [1] B. Gutenberg and C. F. Richter, *Ann. Geophys.* **9**, 1 (1956).
  - [2] J. Schmittbuhl and K. J. Maloy, *Phys. Rev. Lett.* **78**, 3888 (1997).
  - [3] T. H. Heaton, *Phys. Earth Planet. Inter.* **64**, 1 (1990).
  - [4] J. Carlson and S. B. Nielsen, in *EOS Transactions* (American Geophysical Union, Washington, D.C., 1998), No. 45, p. F643.
  - [5] D. S. Fisher, K. Damien, S. Ramanathan, and Y. Ben-Zion, *Phys. Rev. Lett.* **78**, 4885 (1997).
  - [6] R. Burridge and L. Knopoff, *Bull. Seismol. Soc. Am.* **57**, 3411 (1967).
  - [7] H. Larralde and R. C. Ball, *Europhys. Lett.* **30**, 87 (1995).
  - [8] C. R. Myers, B. E. Shaw, and J. S. Langer, *Phys. Rev. Lett.* **77**, 972 (1996).
  - [9] J. M. Carlson and A. A. Batista, *Phys. Rev. E* **53**, 4153 (1996).
  - [10] If the coefficient of friction  $\mu$  is velocity or slip dependent, the only change to first order in the speed of the boundary, is in the coefficient of the left hand side of Eq. (2).
  - [11] In fact, when  $T > \gamma$ , there is a propagating mode in the velocity fluctuations of the boundary for  $\mu$  greater than a critical value. This mode can be excited by any heterogeneity in the friction constant or spatial variations in the driving load. Thus the physics even above the threshold load  $\gamma$  should be interesting.

- [12] S. Ramanathan and A. E. Lobkovsky (unpublished).
- [13] S. Ramanathan and D. S. Fisher, Phys. Rev. Lett. **79**, 877 (1997).
- [14] When the symmetry of the problem is such that one component of the displacement field remains decoupled from the others, acoustic like kernels with  $J(z, t) \sim \frac{t}{z^2} \frac{1}{(t^2 - z^2)^{1/2}}$  arise for the equations of motion of these components, as that for a crack front under tearing loading or the component of the displacement transverse to the direction of the shear in the case of friction. There are two necessary conditions for elastodynamics to give rise to kernels with property (iii). First, the co-dimension of the elastic interface has to be spanned by components of the displacement field. And second, the displacement field components along the boundary must not be decoupled from the bulk.
- [15] D. Ertas and M. Kardar, Phys. Rev. E **49**, R2532 (1994).
- [16] A. A. Middleton, Phys. Rev. Lett. **68**, 670 (1992).
- [17] S. Ramanathan and D. S. Fisher, Phys. Rev. Lett. **79**, 877 (1998).
- [18] S. Nielsen, private communication (unpublished).

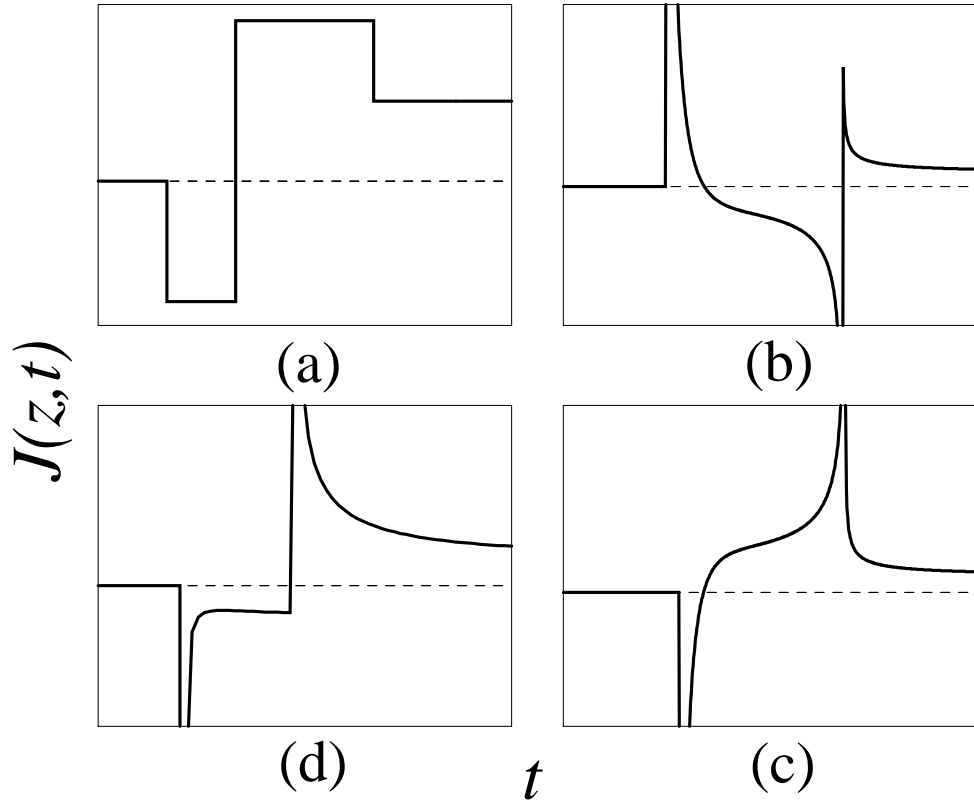


FIG. 1. Kernel  $J(z, t)$  at position  $z$  as a function of time  $t$ . Model kernel (a) represents essential features of kernels that arise in fracture (b) and solid on solid friction (c) and (d). Graph (c) is for  $z < 0$ , (d) is for  $z > 0$ . The friction coefficient is  $\mu = 3$ .

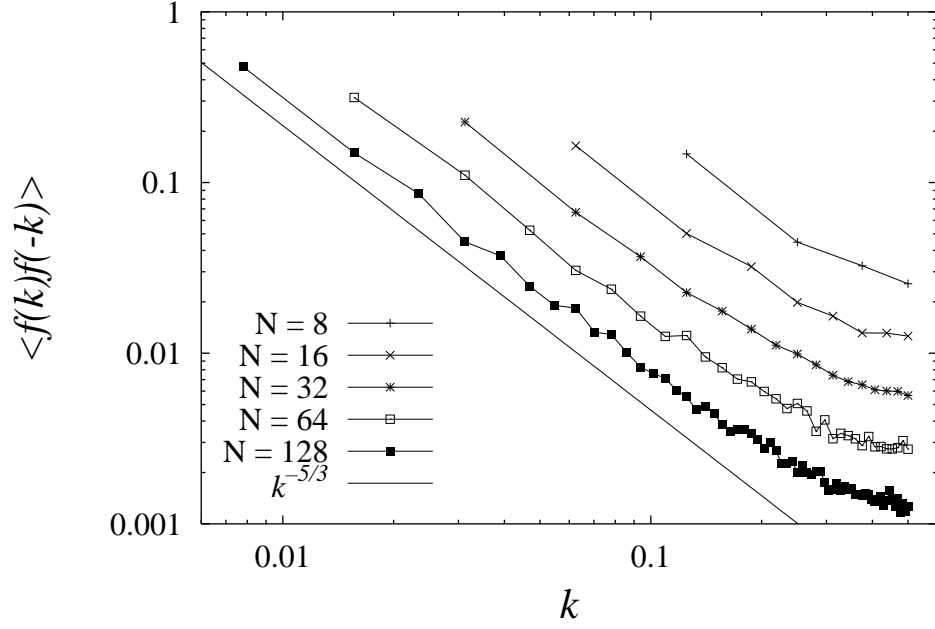


FIG. 2. Boundary statistics  $\langle f(k)f(-k) \rangle$  just before it begins to move for the model kernel with no bump ( $\alpha = 0$ ). The solid line is the  $k^{-5/3}$  scaling expected from the renormalization group arguments. Length are measured in terms of the correlation length of the randomness.

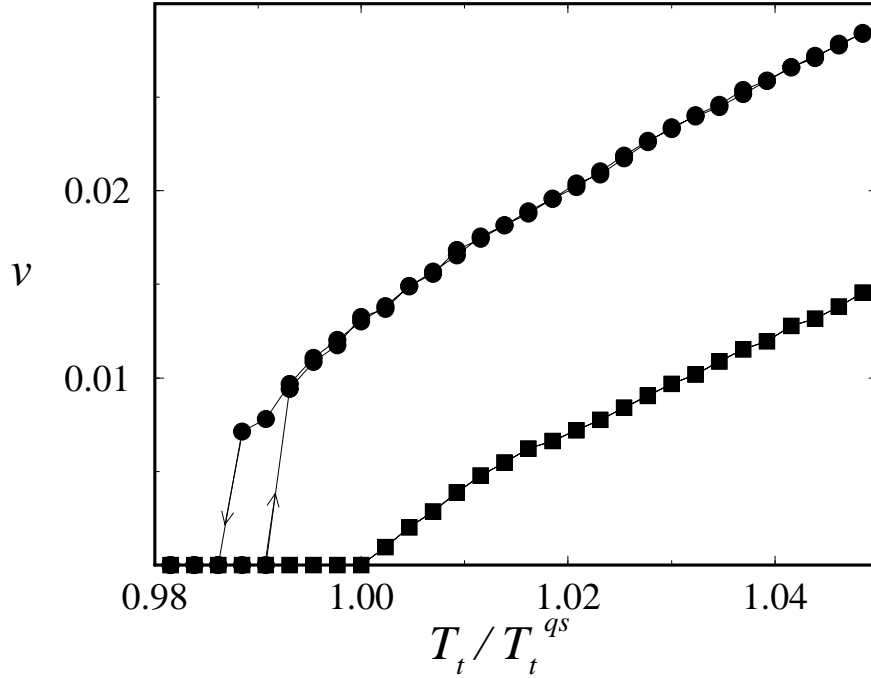


FIG. 3. Average boundary velocity  $v$  in units of the fastest wave speed as a function of the applied driving  $T$  in units of the quasistatic threshold load. The model kernel with  $\alpha = 0$  data is plotted with squares. When  $\alpha > 0$  (circles) the velocity is discontinuous and hysteretic.

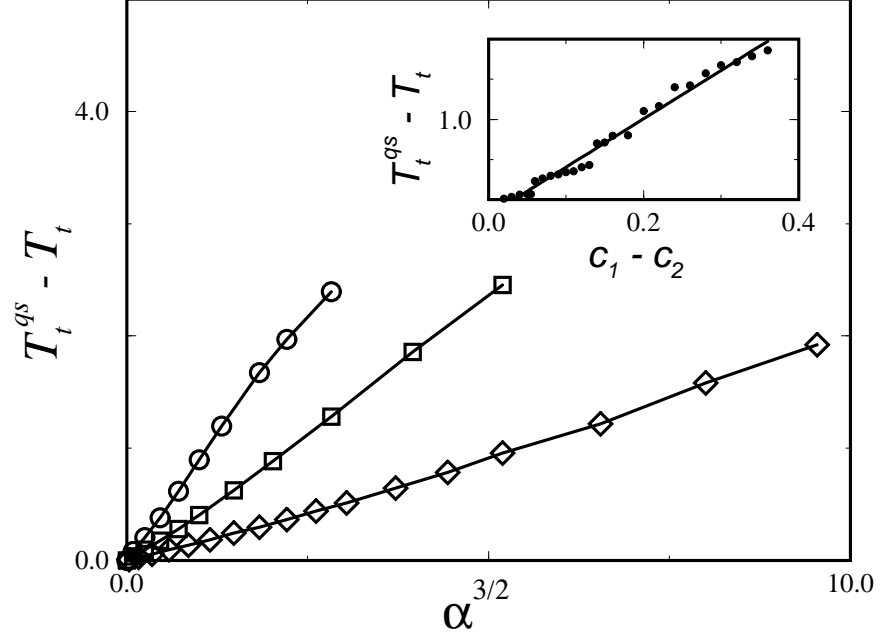


FIG. 4. Threshold force suppression for the model kernel with respect to the quasistatic value versus the  $3/2$  power of the bump height  $\alpha$ . The forces  $T$  are in natural units. Diamonds correspond to  $c_2 = 0.417$ , squares to  $c_2 = 0.333$ , and circles to  $c_2 = 0.2$ . The inset shows the threshold force as function of the  $c_1 - c_2$ . In both graphs  $c_1 = 0.5$  is fixed.